On the modelling of pore pressure developments below cyclically loaded offshore gravity foundations

Martijn van Wijngaarden[*†]

Saturated sands show an increase in pore pressure under cyclic loading in undrained conditions. A challenge in modelling pore pressures below offshore gravity foundations is the effect of random or irregular cyclic loads. In literature, a method is proposed in which equivalent loads with a constant period and a constant amplitude are used. In this paper, a method is presented which takes both the irregular nature of cyclic loads and the real load development in time into account. The cyclic loads are derived in the frequency domain for a gravity foundation of an offshore wind turbine. The irregular loads are simulated with a random phase model. The pore pressures are modelled in a one-dimensional model including three-dimensional dissipation. The results show that the irregular nature of the cyclic loads results in a significant spread in maximum pore pressures below the foundation.

Keywords: Pore pressure, Cyclic loads, Gravity foundation, Offshore, Wind, Modelling

Introduction

Offshore foundations are exposed to cyclic loads generated by waves. Offshore foundations of wind turbines are also exposed to cyclic wind loads. For wave-loaded gravity foundations, the effect of cyclic shear forces at seabed level is dominant. For a gravity foundation of an offshore wind turbine, also cyclic bending moments at the seabed level should be taken into account, due to the large turbine heights. The paper will focus on a gravity-based foundation for an offshore wind turbine placed on medium-dense sand, although the proposed method can also be applied to offshore foundations that are only loaded by waves.

Multiple cases are known from literature in which vertical caisson breakwaters collapsed due to a rapid increase in pore pressures below the caisson (Oumeraci 1994). Pore pressures may have a significant effect on the stability of an offshore gravity foundation for an offshore wind turbine as well. Currently, the design is often based on the static stability check, while the relation between cyclic loading of the subsoil and the stability of the structure receives less attention (Safinus, Sedlacek, and Hartwig 2011; Det Norske Veritas (DNV) 2014).

Saturated sands show an increase in pore pressure under cyclic shear loading in undrained conditions (Seed and Rahman 1978; Rahman and Jaber 1986). The main parameters influencing the increase in pore pressure are the relative density of the sand and the permeability of the sand. Denser-packed sands show less contraction under cyclic loading in undrained conditions compared to loosely packed sands, resulting in less pore pressure build-up. The pore pressures will dissipate in partly drained conditions. The amount of dissipation depends on the permeability of the sand and is influenced by the particle size distribution. Sands densify due to the dissipation of pore water and consequently show less pore pressure build-up under further cyclic loading since less contraction occurs in denser-packed sands. The dissipation of pore pressures and the resulting densification can be seen as an increase in resistance to further pore pressure generation. Sands also form a stronger packing structure under partly drained cyclic loading. This strengthening effect of sands is an addition to the explained strengthening due to densification (Meijers and Luger 2012), and is named preshearing or history effect.

The seabed preparation has a significant effect on the pore pressure regime. A gravel bed is often installed below the gravity foundation. A gravel bed provides a horizontal drainage layer below the foundation and results in lower pore pressures compared to a gravity foundation directly placed on the seabed. The size of the baseplate also influences the rate of pore pressure dissipation. A larger baseplate increases the length of the drainage path and reduces the rate of dissipation.

Faculty of Civil Engineering and Geosciences, Delft University of Technology, Delft, Netherlands

*Corresponding author, email mjpvanwijngaarden@gmail.com

†Currently Trainee at Volker Staal en Funderingen b.v., Rotterdam, Netherlands.

Received 29 October 2017; accepted 13 April 2018
DOI 10.1080/19375247.2018.1467070

In this paper, the influence of a gravel bed and the size of the baseplate is not further investigated. A circular gravity foundation with a diameter of 30 m is investigated, placed on a homogeneous sand profile without a top layer with a high permeability.

The main processes of cyclically loaded offshore gravity foundations for a wind turbine are indicated in Fig. 1. The cyclic loads consist of wind loads, turbine loads, wave loads and dynamic amplification of all of the loads. The processes in the subsoil are pore pressure generation, dissipation and consolidation. The increase in pore pressure above the originally present pore pressure is called the excess pore pressure (EPP). The dissipation of EPPs might affect the stability of the foundation due to settlement and tilting, though might also affect the stability of the scour protection, eventually also affecting the structural stability.

Challenges in modelling EPPs

Pore pressures can be divided into instantaneous and residual pore pressures. The instantaneous pore pressures fluctuate with the hydrostatic pressure of a wave travelling over the structure. The residual pore pressure gradually increases or decreases during cyclic loading due to contraction of the sand and dissipation of pore pressures. The focus in this paper is on residual pore pressures.

In various research projects, cyclic loads are often based on a schematised design storm in which wave heights gradually increase and decrease again (Oumeraci 1994; De Groot, Kudella, Meijers, and Oumeraci 2006; Kudella, Oumeraci, De Groot, and Meijers 2006). The wave loads are schematised in parcels of equal amplitude and equal period, resulting in regular load time series. The design storm is often further simplified into an equivalent storm with fewer load parcels, to minimise the number of computations. However, in reality, the storm does not look like a schematised storm with parcels of equal wave height. The resulting EPPs will also be different since soil properties such as density and permeability will continuously change due to the dissipation of pore pressures and densification of the subsoil.

The main challenges in modelling EPPs are summarised:

- *The load history.* Under cyclic loading, the properties of the subsoil below an offshore gravity foundation continuously change due to effects of dissipation of pore pressures and densification. Faccioli (1973) proposed an empirical relationship between the relative density of sand and the strength in terms of the number of load cycles to full liquefaction, based on cyclic simple shear tests with constant load amplitude:

$$\frac{\Delta\tau_c \,/\, \sigma'_{v0}}{I_d} = a \times N_{liq}^{-b},$$

where $\Delta\tau_c$ is the cyclic shear stress amplitude (kPa); σ'_{v0} is the initial vertical effective stress (kPa); I_d is the relative density (–); N_{liq} is the number of load cycles up to liquefaction (–) and a, b is the empirical constants (–). The relationship is plotted in Fig. 2 for various relative densities. It shows that an initially denser-packed sand has less pore

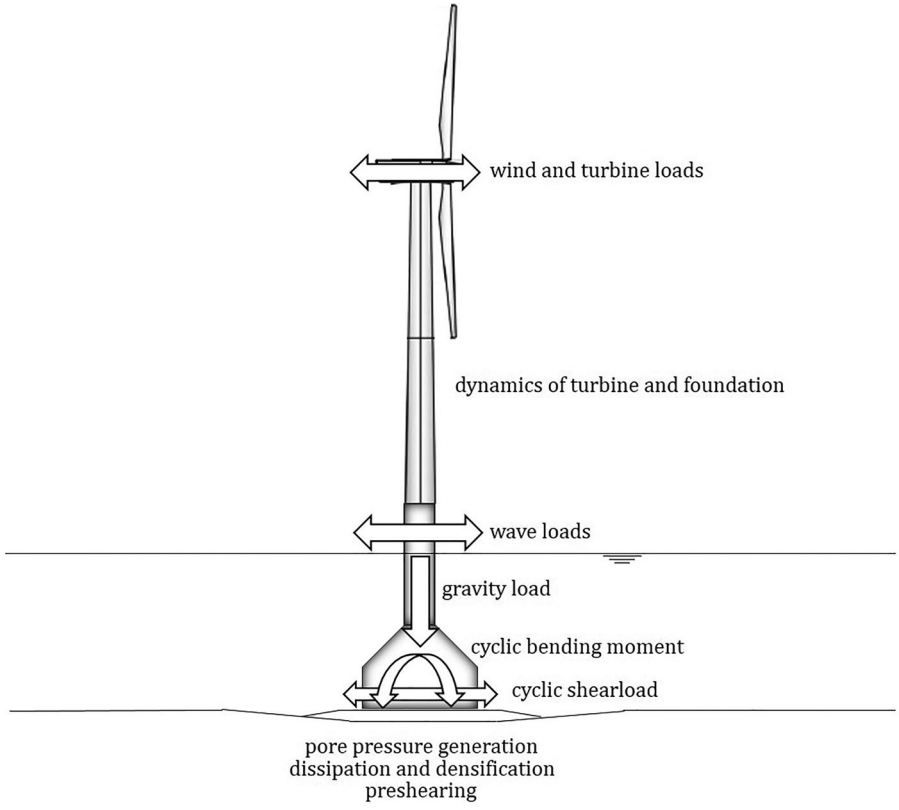

1 Main processes when considering cyclic loads on an offshore gravity foundation for a wind turbine

pressure generation than a loosely packed sand, at least in undrained conditions with the same cyclic load amplitude. Densification results in a larger number of cycles up to liquefaction if the cyclic load amplitude remains constant. Therefore, the load history plays a major role in the maximum pore pressure that is reached during the lifetime of the foundation.

- *The number of load cycles.* An offshore foundation is exposed to a large number of load cycles in the total lifetime. This results in a large calculation time in constitutive soil models. Furthermore, the numerical error increases in each modelled load cycle, resulting in a less reliable pore pressure output. Safinus *et al.* (2011) concluded that the number of load cycles in a constitutive model should not exceed 100 to limit the numerical error. For wave loads, this represents only a small part of a storm and therefore a full constitutive model is not suitable to model a large number of load cycles. Instead, the modelling can be based on an empirical model with input from laboratory tests. Empirical models, however, lack the ability to model the stress state and the local drainage paths during cyclic loading.
- *The random or irregular nature of the loads.* In current practice, the irregular cyclic loads are transformed into an equivalent cyclic load, based on earthquake engineering (Seed and Rahman 1978). The equivalent load is defined as the load that results in a similar soil response as the irregular load. The soil and pore pressure response, however, largely depends on the irregular cyclic loads since the processes of pore pressure generation, dissipation and densification lead to continuously changing soil properties in time.

Meijers, Raaijmakers, and Luger (2014) showed the differences between regular and irregular wave loading on modelled EPPs in a horizontal seabed in a water depth of 10 m. A regular and an irregular wave loading were compared, both with a significant wave height of 6 m and a wave period of 9 s. A relative density of the seabed of 50% is used and a permeability of 0.5×10^{-4} m/s. The pore pressure output is shown in Figs. 3 and 4 at a depth of 1 m below seabed level.

The results show that each of the five irregular time series results in another maximum value of EPP. The spiky pattern of EPPs in Fig. 4 is the result of differences in individual wave amplitude and wave period in the irregular loading, which is not present in the case of regular wave loading in Fig. 3.

The mentioned challenges in the modelling of EPPs are taken into account in this paper.

General approach

EPPs are evaluated for a 30-m diameter gravity foundation for an 8 MW offshore wind turbine (Vestas Wind Systems 2012) placed on medium-dense sand. The first step is the derivation of wind loads on the turbine and waves loads on the foundation. The loads are derived in the frequency domain. The real storm load history of 49 years at the location of an offshore demonstrator project (Weisse, Von Storch, and Feser 2005) is used to capture real load histories instead of schematised load parcels. The derived cyclic loads are used in the empirical model of Seed and Rahman (Rahman and Seed 1977), which is able to take a large number of load cycles into account. The subsequent paragraphs explain the method in more detail.

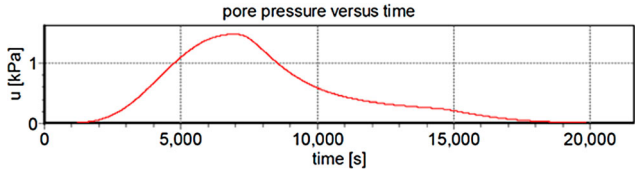

3 pore pressure development over time for regular wave loading (from Meijers and Luger 2012)

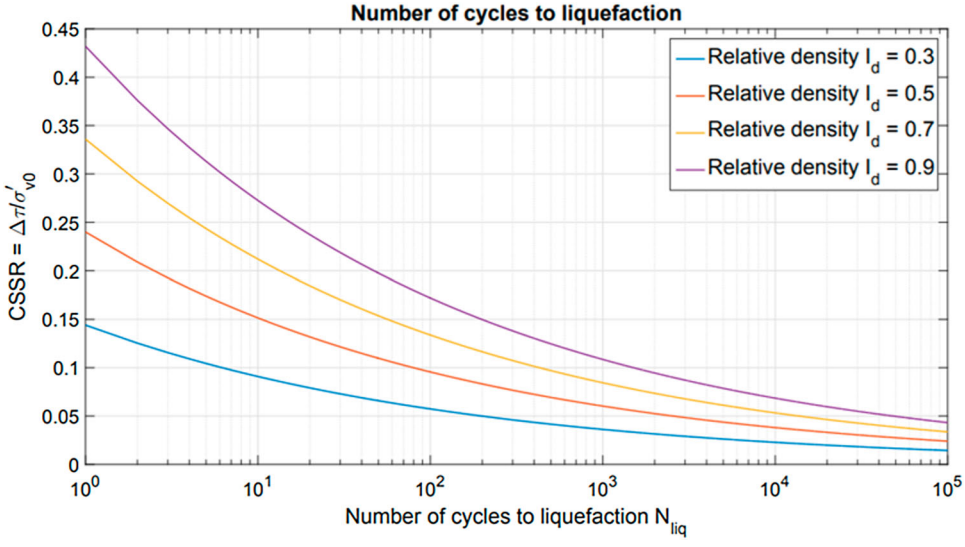

2 The relative density and the CSSR determine the number of cycles to full liquefaction

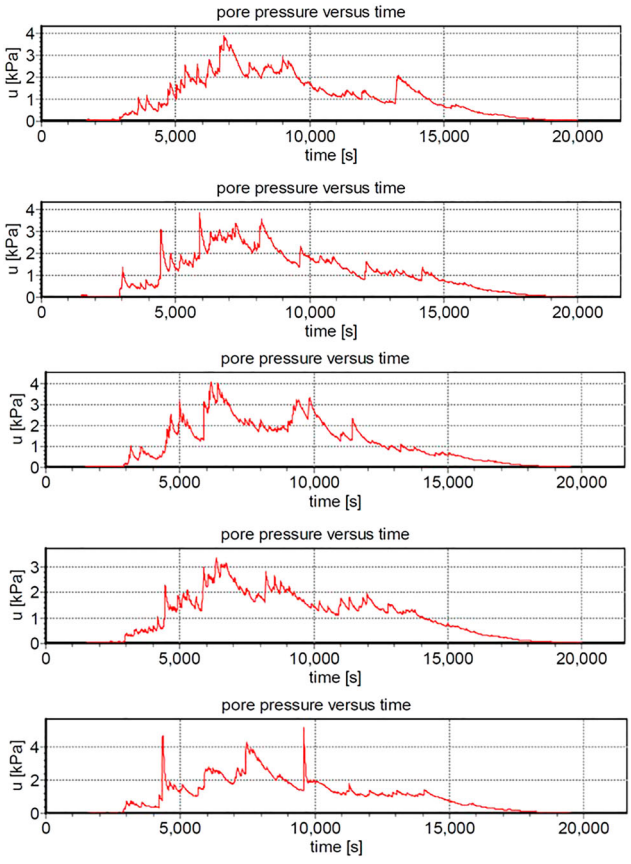

4 Pore pressure development over time for five irregular wave pressure time series (from Meijers and Luger 2012)

Cyclic loading of the subsoil

The cyclic loads in the subsoil are calculated based on a cyclic shear load and a cyclic bending moment at seabed level. This is based on the procedure in Rahman and Seed (1977). The cyclic loads in the subsoil are expressed in cyclic shear stress ratio's (CSSR) values, defined as cyclic shear stress divided by initial vertical effective stress:

$$\mathrm{CSSR} = \frac{\Delta\tau_c}{\sigma'_{v0}},$$

where CSSR is the cyclic shear stress ratio (–); $\Delta\tau_c$ is the cyclic shear stress amplitude (kPa) and σ'_{v0} is the initial vertical effective stress (kPa).

The CSSR values are calculated for the load cycle with the maximum load amplitude in the dataset of storm data of 49 years. In this load cycle, the loads from wind, turbine and waves in terms of shear forces and bending moments at seabed level are included. The CSSR values are calculated in a constitutive model assuming that the sand behaves undrained during the load cycle with maximum amplitude. The undrained behaviour may not be realistic for the top soil layers. However, the pore pressure development in the maximum load cycle is negligible. The maximum CSSR values below the gravity foundation are calculated following the method in Boeije, De Groot, and Meijers (1993). The CSSR values are used in the modelling of pore pressure developments, after deriving the cyclic loads in the frequency domain.

Loads at seabed

The cyclic loads are characterised by the amplitude and the frequency. The amplitude and frequencies of the wind, wave and turbine loads at seabed level are expressed in a spectrum of shear forces and bending moments. A Kaimal spectrum is used for wind loads and a JONSWAP spectrum is used for wave loads in the North Sea (Det Norske Veritas (DNV) 2014). A total spectrum of shear forces and bending moments at seabed level is found by combining the spectra of individual loads (Arany, Bhattacharya, Macdonald, and John Hogan 2015). Load time series can be generated from the spectra using an inverse Fourier transform. A random phase is added to the time series to simulate the random or irregular nature of the loads (Van der Tempel 2006).

A system loaded with a signal with amplitude F can be analysed in the frequency domain with a Fourier transformation. This results in a load input spectrum $S_f(f)$. The system itself can be analysed in the frequency domain by analysing its response A to loads with different frequencies. This results in a response spectrum of the system $S_A(f)$. The spectra can be linked with a Transfer Response Function (TRF). If the TRF is known, the response of the foundation to each load input spectrum can be analysed in the frequency domain. The signal can subsequently be transformed into the time domain with an inverse Fourier transform (Van der Tempel 2006). After adding a random phase to the time signal, each summation of frequencies and amplitudes results in a different time signal:

$$F_t = \sum_{f=1}^{\mathrm{end}} A_f \sin(2\pi f_f t + \varphi_f),$$

where F_t is the load signal in time (N); A_f amplitude of load signal f (N); f_f is the frequency of load signal f (Hz); and φ_f is the phase of load signal f (rad).

The approach is presented for the wind loads. The wind speed is expressed in the frequency domain with a Kaimal spectrum, representing wind speeds versus frequency (International Electrotechnical Committee (IEC) 2014):

$$S_{uu}(f) = \sigma_u^2 \frac{4(L_k/\bar{U})}{(1 + 6f(L_k/\bar{U}))^{(5/3)}},$$

where S_{uu} is the Kaimal spectrum, spectral density of wind speed ((m/s)^2/Hz); σ_u is the standard deviation of wind speed (m/s); L_k is the integral length scale (m); f is the frequency (Hz); $\bar{U}$ is the 10-min averaged wind speed (m/s) and $\sigma_u = \bar{U}I$, with I the turbulence intensity (–).

The recommended theoretical reference turbulence intensity, as described by the IEC, is used in this study. The thrust force on the turbine is related to the wind speed by a frequency independent thrust coefficient:

$$F_{\mathrm{thrust}} = \frac{1}{2}\rho A C_T U^2,$$

where F is the thrust force on turbine (N); ρ is the density of

air (kg/m^3); A is the rotor swept area (m^2); C_T is the thrust coefficient (–) and U is the wind speed.

The wind speed consists of a mean and a fluctuating part. The wind load consists of a mean ($\bar{U}$) and a fluctuating part (u) as well:

$$F_{\text{thrust}} = \frac{1}{2}\rho A C_T(\bar{U}^2 + 2\bar{U}u + u^2) \approx \frac{1}{2}\rho A C_T \bar{U}^2 + \rho A C_T \bar{U}u.$$

The spectral density is defined as the amplitude squared divided by the frequency interval (Arany *et al.* 2015). It can be obtained by multiplying the squared dynamic amplitude of the thrust force with the normalised Kaimal spectrum. The normalised Kaimal spectrum is the Kaimal spectrum divided by the standard deviation squared. If the fluctuating part of the wind speed is approximated by the standard deviation, the resulting spectrum is:

$$S_{\text{ff,wind}} = (\rho A C_T \bar{U}u)^2 \bar{S}_{\text{uu}}(f) = \rho^2 A^2 C_T^2 \bar{U}^4 I^2 \bar{S}_{\text{uu}}(f)\,,$$

where

$$\bar{S}_{\text{uu}}(f) = \frac{S_{\text{uu}}}{\sigma_u^2},$$

where $S_{ff,\text{wind}}$ is the spectral density of horizontal force at seabed level due to wind loads (N^2/Hz); S_{uu} is the Kaimal spectrum: spectral density of wind speed ((m/s)^2/Hz); $\bar{S}_{\text{uu}}(f)$ is the normalised Kaimal spectrum (1/Hz); σ_u is the standard deviation of wind speed (m/s).

This spectrum represents the horizontal shear force at seabed level, generated by the horizontal wind loads on the wind turbine. The spectrum of bending moments at seabed level is found by multiplying with the turbine height above the seabed. Cyclic loads from waves on the foundation and cyclic loads from the operating turbine can be included in a similar manner. Dynamic amplification is also included and is based on the proposed method by DNV (Det Norske Veritas (DNV) 2014).

Load spectra

The wind and wave data at a demonstrator site for offshore wind foundations is used to generate load spectra (Weisse *et al.* 2005). Spectra of shear forces and bending moments at seabed level are derived as a function of time in a storm (Fig. 5). Time series are subsequently generated from the spectra. Owing to the random phase of the time signal, each of the generated time series is different, representing the irregular nature of the loads. The load amplitudes and the zero-crossings are determined in the generated time series (Fig. 6).

Modelling EPPs

The next step in the modelling of EPPs is combining the CSSR values in the subsoil during an extreme load cycle, and the time series of cyclic loads at seabed level. This way of modelling is an explicit approach and does not capture any redistribution of stresses during pore pressure generation and dissipation. A redistribution of stresses below the foundation will result in lower CSSR values and lower EPPs. This is not taken into account in the explicit approach and therefore conservative values of EPPs are found.

The EPPs are calculated with the programme DCycle. The previously mentioned processes of pore pressure generation, dissipation and densification are implemented in this in-house model of the research institute Deltares, as described in Meijers and Luger (2012). The basis of the programme is the one-dimensional vertical consolidation equation, extended with a horizontal consolidation term for an axial-symmetric structure such as a circular gravity foundation:

$$\frac{\partial u}{\partial t} = A(z, t) + c_v \frac{\partial^2 u}{\partial z^2} + c_h\left(\frac{1}{r}\frac{\partial u}{\partial r} + \frac{\partial^2 u}{\partial r^2}\right),$$

where u is the EPP (kPa); z is the vertical coordinate (m); c_v, c_h are the vertical and horizontal consolidation

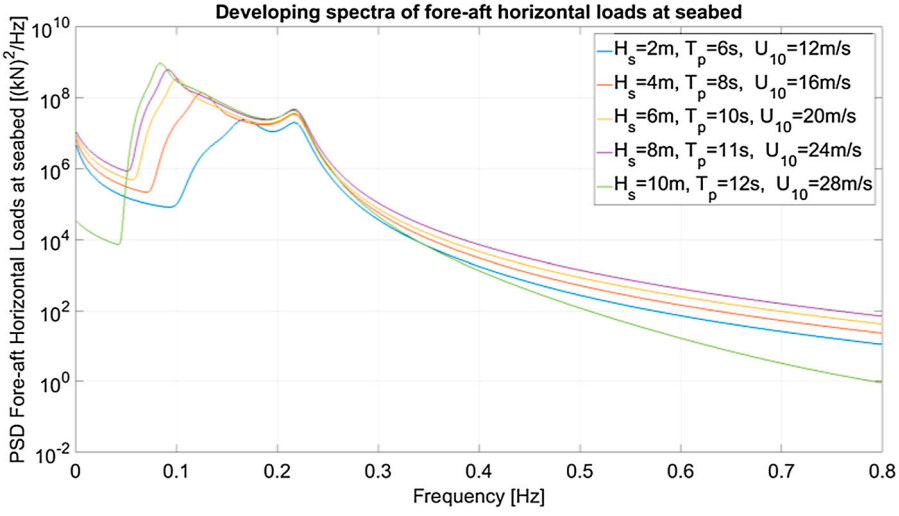

5 Spectra of horizontal loads at seabed level for various significant wave heights, wave periods and wind speeds

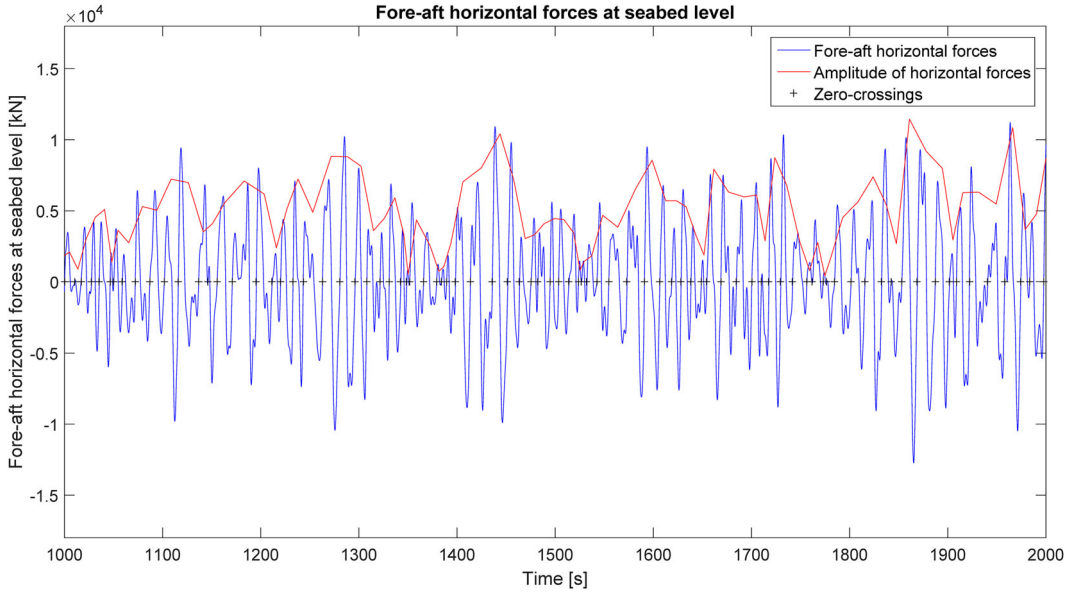

6 Load cycles are analysed by their period (from zero-crossings) and by the amplitude

coefficients (m^2/s); r is the radial coordinate from the centre of the gravity foundation (m).

The pumping or generation term A is represented by the model of Seed and Rahman (1978):

$$r_u = \frac{2}{\pi}\sin^{-1}\left(\frac{N}{N_{liq}}\right)^{(1/2\theta)},$$

where r_u is the relative EPP:ratio of EPP over initial vertical effective stress (–); θ is the rate of pore pressure increase, 0.7 for sands (–); N is the number of load cycles (–); and N_{liq} is the number of load cycles up to full liquefaction (in undrained conditions) (–).

The consolidation coefficient depends on the stress state and the relative density. The DCycle model has been extended with a user-defined cyclic load input in terms of amplitudes and frequencies of individual load cycles (Meijers *et al.* 2014). The CSSRs are scaled with the ratio of the load amplitude in each load cycle over the maximum load amplitude.

Results

Some results of the proposed method of modelling pore pressures are presented in this section. The results are calculated for a homogeneous sand profile with a relative density of 60%. The on-average highest pore pressures are shown in Fig. 7 based on the wind and wave data in the dataset. The horizontal shear force amplitudes at seabed level are presented as hourly averaged values on the left vertical axis since each of the generated time series of loads is different due to the random phase model. Three EPP curves are calculated at seabed level below the centre of the gravity

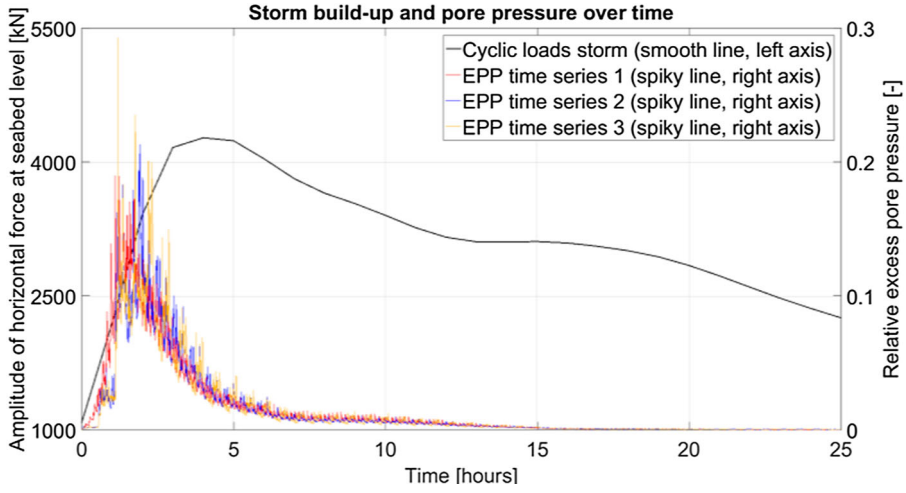

7 Three random realisations of the hourly averaged cyclic load amplitude (smooth line, left axis) are generated and the resulting EPP curves are plotted (spiky lines, right axis)

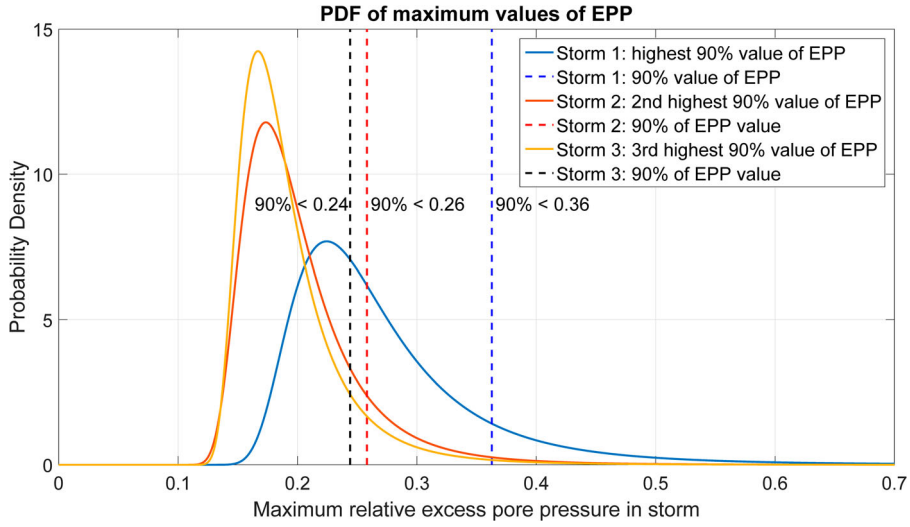

8 For three storms the 90% values in maximum EPPs are shown. The probability density function (PDF) of pore pressures is plotted based on 200 generated time series for each of the storms. The storms include cyclic loads from wind, wave and turbine

foundation, based on three randomly generated time series of the storm. The EPP curves are plotted on the right axis.

The pore pressure varies with the cyclic load cycles, resulting in a spiky development over time. In the first hour of the storm, the EPP increases due to the increasing cyclic load amplitude. After a few hours, when dissipation of pore pressure increases, the soil starts to densify. This results in less pore pressure generation in subsequent load cycles and in a decreasing pore pressure curve, even before the maximum load amplitude has been reached.

The results show that each of the time series results in a different maximum value of EPP in the storm. With a single calculation, no reliable estimate of the maximum EPP can be obtained. The irregular nature of the loads must be taken into account, instead of a load time series with regular loads. Furthermore, it is necessary to make a large set of calculations for each storm in the dataset to derive an EPP value with a certain probability of exceedance.

The storms with the largest EPPs are shown in Fig. 8. For each storm, a set of 200 irregular load time series is generated. A distribution of maximum values of EPPs is made for each of the storms. Based on a 90% value of the EPP distribution, representing an upper limit which is only exceeded during 10% of the load time series, an EPP is found that may be used for the stability assessment of the offshore gravity foundation.

Concluding remarks

In this paper, the challenges in modelling EPPs are identified. An approach is presented to take the effects of irregular cyclic loads into account in the pore pressure developments. Real load histories are used based on a dataset consisting of wind and wave data on the location of an offshore demonstrator project. Loads from wind, wave and turbine are taken into account with a load derivation in the frequency domain. With the dataset, the spectra are calculated for various storms in the lifetime of the foundation. A random phase model is used to represent the irregular nature of cyclic loads.

The EPPs are calculated in the programme DCycle. The results clearly show that it is not possible to present a reliable estimate of the maximum EPP by only considering a single load time series. Based on a large set of generated time series, a value for the EPP can be obtained with a certain reliability (i.e. a 90% value). In this study, the method has been applied to a gravity foundation for an offshore wind turbine, but the method can be applied to any cyclically loaded offshore gravity foundation.

A further validation of the proposed method is recommended. This may be based on laboratory tests or field measurements. Furthermore, it is recommended to develop a probabilistic approach to obtain a design value of the EPP below a gravity foundation to assess its stability under cyclic loading.

Also a coupling is recommended between the constitutive modelling of soils and the empirical modelling of pore pressures. Although very complex, this coupling is necessary to take a changing stress distribution under cyclic loading into account in EPP calculations. Finally, it is recommended to extend the research to other foundation concepts for offshore wind turbines, such as monopile foundations.

References

Arany, L., Bhattacharya, S., Macdonald, J. and John Hogan, S. 2015. Simplified critical mudline bending moment spectra of offshore wind turbine support structures. *Wind Energy*, **18**, 2171–2197.

Boeije, R. P., De Groot, M. B. and Meijers, P. 1993. Pore pressure generation and drainage underneath gravity structures. *International Offshore and Polar Engineering Conference*.

De Groot, M. B., Kudella, M., Meijers, P. & Oumeraci, H. 2006. Liquefaction phenomena underneath Marine gravity structures subjected to wave loads. *Journal of Waterway Port, Coastal, and Ocean Engineering*, **132**, 325–335.

Det Norske Veritas (DNV). 2014. Design of offshore wind turbine structures (DNV-OS-J101).

International Electrotechnical Committee (IEC). 2014. NEN-EN-IEC 61400-2, Wind turbines - Part 2: small wind turbines.

Faccioli, E. 1973. A stochastic model for predicting seismic failure in a soil deposit. *Earthquake Engineering and Structural Dynamics*, **1**, 293–307.

Kudella, M., Oumeraci, H., De Groot, M. B. and Meijers, P. 2006. Large-scale experiments on pore pressure generation underneath a Caisson breakwater. *Journal of Waterway Port, Coastal, and Ocean Engineering*, **132**, 310–324.

Meijers, P. and Luger, D. 2012. On the modelling of wave-induced liquefaction, taking into account the effect of preshearing. *Proceedings of Twenty-second (2012) International Offshore and Polar Engineering conference*, **2**, 739–745.

Meijers, P., Raaijmakers, T. and Luger, D. 2014. The effect of a random wave field on wave induced pore pressure feneration. *Proceedings of the Twenty-fourth (2014) International Ocean and Polar Engineering Conference*, **3**, 668–675.

Oumeraci, H. 1994. Review and analysis of vertical breakwater failures. *Coastal Engineering*, **22**, 3–29.

Rahman, M. and Jaber, W. Y. 1986. A simplified drained analysis for wave-induced liquefaction in ocean floor sands. *Soils and Foundations*, **26**, 57–68.

Rahman, M. and Seed, H. 1977. Pore pressure development under offshore gravity structures. *Journal of Geotechnical Engineering*, **103**, 1419–1436.

Safinus, S., Sedlacek, G. and Hartwig, G. 2011. Cyclic response of granular subsoil under a gravity base foundation for offshore wind turbines. *Proceedings of the International Conference on Offshore Mechanics and Arctic Engineering*, **7**, 875–882.

Seed, H. and Rahman, M. 1978. Wave-induced pore pressure in relation to ocean floor stability of cohesionless soils. *Marine Geotechnology*, **3**, 123–150.

Van der Tempel, J. 2006. *Design of support structures for offshore wind turbines*. PhD, Delft University of Technology.

Vestas Wind Systems. 2012. Vestas V164 8.0 MW.

Weisse, R., Von Storch, H. and Feser, F. 2005. Northeast Atlantic and North Sea storminess as simulated by a regional climate model during 1958–2001 and comparison with observations. *Journal of Climate*, **18**, 465–479.